Application of Multisensor Data Acquisition in Reservoir Heterogeneity

Min Li(✉)

Daqing Oilfield Limited Company, No. 4 Oil Production Company, Daqing 163511, China
935748819@qq.com

Abstract. The triadic compound flooding test of three types of oil layers in the North East block of Lamadian oilfield is a key test project of tertiary oil production in Daqing Oilfield. The test area is planned to be put into operation in 2011. Through the analysis of logging data of 32 newly drilled oil wells in the experimental area, the heterogeneity of the layers, interlayer and plane and the influence on the remaining oil are studied. According to the water flooded condition of the reservoir in the test area, the types and distribution of remaining oil are analyzed, The results show that the reservoir conditions of high II 1–18 in polymer flooding test area of three types of reservoirs are compared. Combined with the design and experience of polymer flooding test parameters, it can provide important guidance for the design of three-dimensional test parameters of three types of oil layers.

Keywords: Keywords three types of reservoir · ASP flooding · Heterogeneity · Remaining oil

1 Sedimentary Characteristics of Test Target Layer

Gaoii reservoir belongs to delta front facies deposition. During deposition, the water environment is relatively deep, mainly composed of stable sheet sand with low permeability. There are many calcareous layers. The color of mudstone is mostly gray green to gray black. The plane of sand body is stable and the difference of heterogeneity is small. The sand bodies of high delta front can be divided into two types of high delta units, i.e., high delta units, high delta units and high delta units.

On the afternoon of September 2, a special video conference on the analysis of the city's economic operation was held [1]. All district and county departments are required to strengthen the research and analysis of main economic indicators, determine the prominent links between prominent contradictions and weak links, strengthen operation scheduling, promote the implementation of various objectives and tasks, and improve the quality and efficiency of economic development.

On the afternoon of July 16, a special dispatching promotion meeting was held to analyze the city's industrial economic operation and accelerate the investment in industrial "technological reform" to cultivate new scale industrial enterprises. Further deploy the leading task of "six comparisons" industry and information technology system

© The Author(s), under exclusive license to Springer Nature Singapore Pte Ltd. 2023
I. Ahmad et al. (Eds.): STSIoT 2021, LNDECT 122, pp. 670–678, 2023.
https://doi.org/10.1007/978-981-19-3632-6_78

and the current urban key industrial economic work, and spare no effort to promote the return of urban industrial economy to a reasonable scope as soon as possible.

The meeting stressed the need to unify thinking, enhance confidence, focus on the municipal Party committee and municipal government, highlight the deployment requirements of industry to break through industry, further take effective measures and strive to overcome difficulties [2]. Ensure that the annual industrial economic growth target is achieved. He analyzed the current economic situation, studied and deployed the next work, and stressed the need to accurately grasp the economic development trend, firmly grasp key areas and key links, and take effective measures to accelerate high-quality development. The following Fig. 1 shows the economic data study of reservoir heterogeneity.

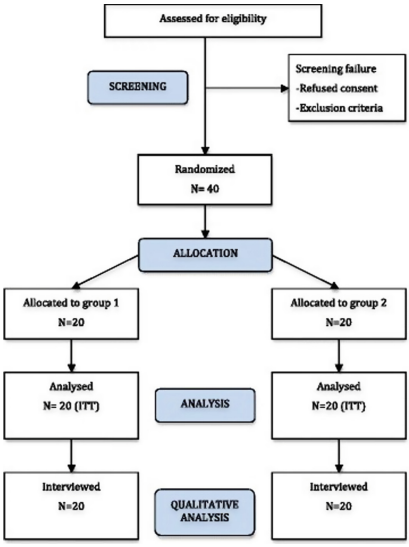

Fig. 1. Study on economic data of reservoir heterogeneity

2 Related Work

In this paper, we aim to application of multisensor data acquisition in reservoir heterogeneity.

Ref [1] reveal that pore type is a crucial cause for strong reservoir heterogeneity of carbonates. Thus, Ref [2] study the effect of wettability heterogeneity and reservoir temperature on the vertical CO2 plume migration, and capillary and dissolution trapping capacities. Accordingly Ref [3] show that the main part of the Mishrif Reservoir is affected by diagenetic processes related to subaerial exposures, resulting in zones with higher storage capacity and fluid flow rates. Petrographic, cathodoluminescence and ultra-violet light fluorescence microscopy analyses of the Arab-D reservoir in an oil field of Saudi Arabia, Ref [4] have been combined with isotope geochemistry (δ13C,

δ18O and 87Sr/86Sr) to decipher the sequence of diagenetic events affecting the reservoir before and during oil emplacements, and the impact of depositional mineralogies and their modifications during the diagenesis on the reservoir quality and heterogeneity [5]. Ref [6] investigate a nonroutine methodology to predict the external and internal distribution of PFUs. These advances provide a platform for introducing a practical approach for introducing the Risk of Commercial Failure (RCF) due to reservoir heterogeneity in hydraulic fracturing projects. Ref [7] define such a parameter and the methodology to calculate it in a time-efficient manner. Ref [8] aim to use electrical image logs in the carbonate Asmari Formation reservoir in Zagros Basin, SW Iran, in order to evaluate natural fractures, porosity system, permeability profile and heterogeneity index and accordingly compare the results with core and well data. Despite its successful application in conventional reservoirs, significant errors arise when extending the concept to unconventional reservoirs. Ref [9] aim to clearly demonstrate such errors when using the traditional square–root–of–time model for DOI calculations in unconventional reservoirs, and to develop new models to improve the DOI calculations. Ref [10] present integrated static reservoir modeling and basin modeling to better characterise the reservoir rock; hydrocarbon-bearing sandstones of the Cenomanian Bahariya Formation.

This paper consists of the following parts. The first part introduces the related background and significance of this paper, the second part is the related work of this paper, and the third part is data analysis. The fourth part is example analysis. The fifth part is conclusion.

2.1 Overview of Data Fusion Theory

Multi sensor data fusion is a new subject developed from 1970s. It has been widely used in C3I system and various weapon platforms. With the rapid development, modern warfare has developed into a five-dimensional structure of land, sea, air, space and electromagnetism. In order to obtain the best combat effect, in modern CI combat system, relying on a single sensor to provide information can no longer meet the demand. It is necessary to use multi-sensor to provide observation data or information, real-time target detection, optimization and comprehensive processing to obtain state estimation The data itself robustness, high measurement dimension, good target space resolution, strong fault tolerance and system reliability Since data fusion was put forward, it has attracted great attention of developed countries and listed it as an important topic in the field of military high-tech research and development [3]. The organize and coordinate systematic research on this key national defense technology, so that in the mid-1980s, data fusion technology first made great progress in the military field.

The observation data of Ruqian sensors obtained in a certain spatio-temporal order are processed under a certain criterion by using computer technology Automatic analysis and synthesis, so as to produce new meaningful data, which can not be obtained by any single sensor.

Today, data fusion technology has been widely used in robotics, traffic management and military fields [4]. At present, the application effect in military field is the most remarkable.

2.2 Reservoir Parameters of Each Well

The plane imbalance is mainly to study the plane distribution characteristics of sand, the flexibility caused by the differences in geometric shape, thickness, continuity and permeability of sand, and the formation and distribution of oil wells.

$$\begin{aligned} &f(t, x_d(t)) + B(t)u_d(t) - f(t, x_k(t)) - B(t)u_k(t) - d_k(t) \\ &= f(t, x_d(t)) - f(t, x_{k+1}(t)) + B(t)\Delta u_{k+1}(t) - d_{k+1}(t) \end{aligned} \tag{1}$$

$$\begin{aligned} &\Delta\dot{x}_{k+1}(t) = P^{-1}(t)(f(t, x_d(t)) - f(t, x_{k+1}(t)) + B(t)\Delta u_k(t) \\ &-\big(B(t)L(t)\dot{C}(t) + B(t)L(t)C(t)\big)\Delta x_{k+1}(t) - d_{k+1}(t)) \end{aligned} \tag{2}$$

Using the reservoir parameters of each well obtained by logging interpretation of 32 newly drilled wells, the thickness contour map of sandstone reservoir sand body unit show that the sandstone thickness of high II 1–18 unit in the test area is larger in the west, smaller in the East and more uniform in the middle; from the perspective of permeability distribution, the distribution is extremely uneven, generally low in the middle and East. From the micro structure distribution map, it is high in the West and low in the East, and there are small undulating structures in the middle. Under the 106 m five point well pattern, the sand body control degree of the effective thickness well points developed in gao∏ 1–18 reservoir in the test area is counted according to the sedimentary unit. The results show that the first class connectivity effective thickness of non channel sand is 97.5%, which is 19.8% and 1.0% test area. Among them, the first class connectivity rate of four-way well pattern is 374%, that of sand body is 63.7%; that of three-way well pattern is 68.6%, that of sand body is 90.1%; that of two-way well pattern is 82.6%, and that of sand body is 97%. Through the analysis of various factors of plane heterogeneity, it is judged that the reservoir in the East is poorly developed, low permeability and prone to residual oil [5].

3 Data Analysis

Interlayer heterogeneity refers to the vertical difference between research units. In the test area, there is a good interlayer condition between Gao 1-18 reservoir. The average thickness of the interlayer is about 1.9 m. There is no adhesive layer between. The average thickness of the upper and lower interlayer is 1.8 m and 1.6 m, respectively.

There are 18 units in the target layer in the test area. According to the oil layer development of each unit, 6 units of Gao II 2, 3, 4 + 5, 12, 13 and 16 are well developed, with large area of channel sand body and remaining oil, which should be the main target of tapping potential. The 4 units of Gao II 1, 9, 182 and 183 are mainly off the surface, with poor reservoir development and less remaining oil. The interlayer heterogeneity in the test area is shown in Fig. 2 below.

Intraformational heterogeneity refers to the vertical change of reservoir properties within a single sand body. It is a key factor that controls and affects the swept volume of injectants and the formation and distribution of remaining oil in a single sand layer [6].

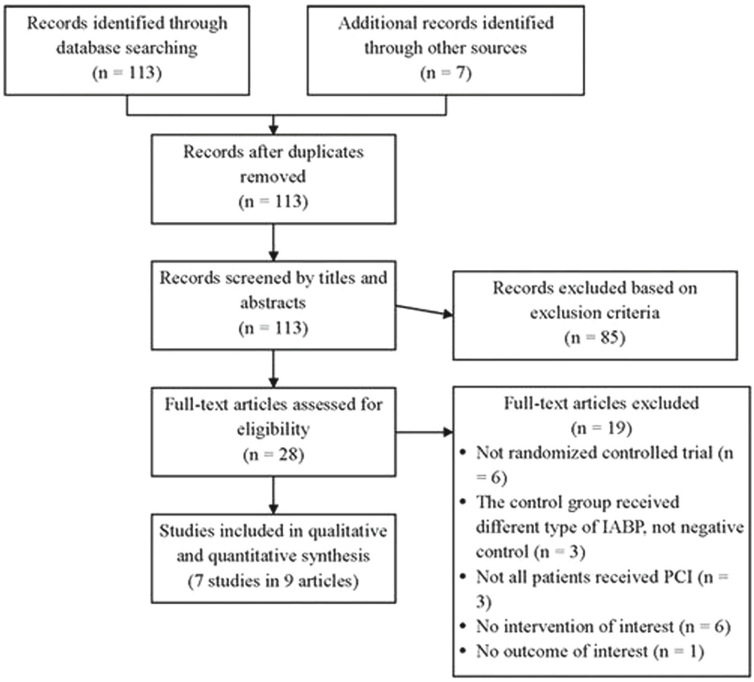

Fig. 2. Interlayer heterogeneity in test area

3.1 Permeability Heterogeneity Model

The high II 1–18 unit is a complex positive rhythm pattern. The permeability at the bottom of the unit is larger than that in the upward direction. However, there are several rhythms of high to low due to the inflow and recession of lake water. Therefore, from the perspective of the whole Gao II 1–18 unit, the rhythm is more complex, and the remaining oil in each unit is different, but on the whole, the remaining oil is less in the lower part and more in the upper part. The complex positive rhythm pattern is shown in Fig. 3 below.

3.2 Improved Neural Network Algorithm and its Application in Reservoir Identification

Multi feedback BP neural network is composed of input layer, output layer and their invisible layer. The input layer receives information from the outside, and the number of nodes in the input layer is the same as the number of variables in the input sample. The output layer transmits the processed information from the network to the outside, and the number of nodes in the output layer is the same as the number of expected parameters. The node excitation function usually selects s function [7].

This paper considers a three-layer feedforward neural network composed of N input units, m hidden units and output units, $x_i (i = 1, \ldots, n)$ is the input of the network,

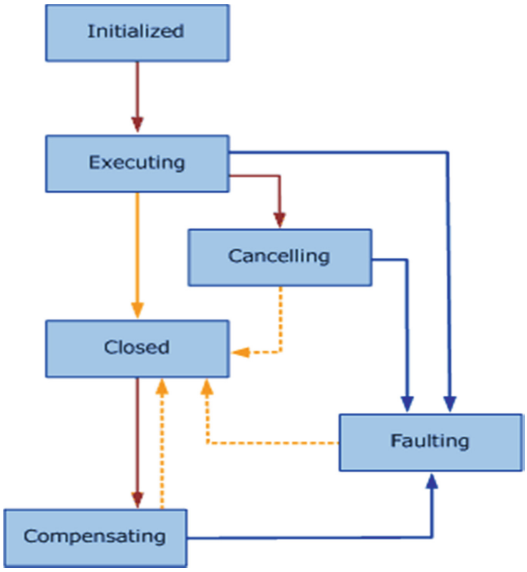

Fig. 3. Complex positive rhythm pattern.

$y_i (j = 1, \ldots, m)$ is the output of the hidden layer, $o_k (k = 1, \ldots, m)$ is the output of the network, and $d_k (k = 1, \ldots, l)$, the expected output). Then there are.

$$o_k = f(net_k) = \left[\sum_{j=0}^{m} w_{jk} f\left(net_j\right) \right] \tag{3}$$

$$y_i = f\left(net_j\right) = f\left(\sum_{j=0}^{m} w_{jk} f\left(\sum_{i=0}^{n} v_{ij} x_i\right)\right. \tag{4}$$

3.3 Interlayer Distribution

Interlayer refers to the heterogeneous layer in the reservoir, which can be divided into physical interlayer, calcareous interlayer and argillaceous interlayer. According to the coring situation of l8-jian182 coring well in the Northeast block, the interlayer of the target layer in the test area is mainly argillaceous interlayer. Usually, the density of interlayer and other parameters are used to reflect the development degree of impermeable interlayer in reservoir, and the distribution of interlayer has great influence on oil-water movement.

Henan Dayou Energy Co., Ltd., Henan Dayou Energy Co., Ltd. The board of directors and all directors of the company guarantee that there are no false records or misleading statements in the contents of this announcement. Internal control has issued a negative opinion audit report, which has been issued a review report on internal control according to the audit report of negative opinion [8]. The stock trading of Shanghai Stock Exchange has begun to be issued, and the stock listing trading of Shanghai Stock Exchange is listed on Shanghai Stock Exchange. From now on, other risk warnings will be implemented.

If the above "secondary" provision is implemented by example, it will be proved to be "five items" in fact. During the warning period of other risks, the company shall issue a reminder notice at least once a month to classify the level. Paragraph discloses the progress of the issues involved. "Paragraph revealed the progress in resolving the matter. A negative audit report was formulated and it was considered that the company violated the provisions of the China Securities Regulatory Commission DiI."

4 Example Analysis

4.1 Water Flooded Condition in the Test Area

According to the statistics of newly excavated oil well inundation data in the test area, high, medium and low water flooded layers of each unit of Gao 1-18 oil layer appear alternately, with obvious multi-stage water flooded characteristics. According to statistics, the thickness ratio of flooded layer is 98.4%, and the thickness ratio of flooded layer is 47.8%. The thickness ratio of high and low water flooded layers is 1:1, and the thickness ratio is about 20.0%. According to the submergence conditions of effective thickness, those with an effective thickness of more than 1.5 m are qualified. The effective thickness between 1.0–1.5 m is secondary water flooded layer, and the high water layer is 56.4%, 12.8% higher than the middle water layer. The proportion of medium water burial is mainly medium water burial, with an effective thickness of 0.5–1.0 m, a thickness of 54.0%, a high water burial of 35.3%, a low water burial of 10.6%. The effective thickness less than 0.5 m is mainly medium water burial, with a proportion of 42.4%, a low water burial of about 39.7%, a high water burial of 15.9%, and a high proportion of non water burial.

According to different permeability and different immersion conditions, the permeability will also reach 0200 μ The store layer larger than M2 is mainly middle and high-rise, and its permeability is 0400 μ The high jellyfish layer larger than M2 accounted for 66.9% and 286% respectively. High, high heavy water leakage rate, high heavy water leakage rate, permeability 0.300–0.00 μ M2 is greater than 40.0%. Heavy water needle accounted for 59.3%, and heavy water needle accounted for 32.6%. The permeability is 0.050–0.00 μ The permeability of M2 is 0.10–0.20 μ The heavy water submergence rate at M2 is 534%, the water storage submergence rate is 345%, and the measurability is 0.05–0.100. μ The heavy water immersion rate of M2 is 38.9%, the water storage immersion rate is 60.3%, and the permeability is 0.050 μ The proportion of reservoirs with less than M2 is 50.0% and 42.5% respectively. From the perspective of tendency, the greater the permeability, the greater the waterproof proportion and the higher the waterproof level [9].

4.2 Uneven Distribution of Oil Saturation

The original oil saturation of gao2 formation is 687%. According to the water flooded interpretation results of new drilling, the oil saturation before the test is 48.5%, which is 2.0% points lower than that in the polymer flooding test area of class III reservoir. According to the distribution of oil saturation, the oil saturation in the east of the test

area is more than 50.0%, 1.5% higher than the average of the whole area, and the remaining oil is rich. Analysis of the reasons, mainly divided into two: 1. See Fig. 4 for the interpretation results of drilling water flooding.

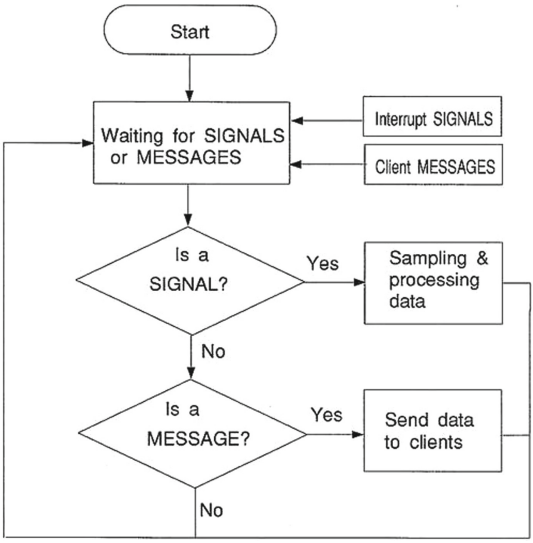

Fig. 4. Interpretation results of drilling water flooding

Earthquake early warning is an important measure of prevention and disaster reduction. The reporter learned that this is the country's first local regulation specifically regulating earthquake early warning, and it is also the "small quick spirit" legislative project of Jiangsu Province this year.

Therefore, it is particularly important to strengthen earthquake early warning management according to law, standardize earthquake early warning activities and play a role. The reporter learned that there are 20 articles in the decision, which mainly stipulate the principles, responsibilities and working mechanism of earthquake early warning, and the responsibilities for the construction, management, release, application and disposal of earthquake early warning system [10]. Information and the guarantee mechanism for earthquake early warning will come into force on January 1, 2022.

Earthquake early warning is based on the principle that the propagation speed of seismic wave is slower than that of electromagnetic wave communication, and the destructive earthquake alarm information is immediately notified to relevant personnel and units through the earthquake warning system. In this regard, Article 2 of the decision stipulates that earthquake early warning "refers to the use of the earthquake early warning system to send earthquake warning information to areas that may be damaged after the occurrence and before the arrival of destructive seismic waves", highlighting earthquakes.

5 Conclusion

Gaoii reservoir belongs to delta sedimentation process, and the water environment is relatively easy. It is mainly composed of stable thin sandwiches with low permeability. There are many lime layers, and the color of mudstone mainly changes from grayish green to grayish black. The plane of sand develops steadily. The imbalance has a great impact on the distribution of remaining oil. The development degree of pond is the main factor determining the distribution of remaining oil in the test area. The reservoirs in the test area are mainly middle and lower reaches and jellyfish, and the remaining oil is unevenly distributed. On the plane, the middle part has high domestic sales and low oil, while the East has low domestic sales and rich oil.

References

1. Liu, H., et al.: Pore types origins and control on reservoir heterogeneity of carbonate rocks in middle Cretaceous Mishrif Formation of the West Qurna oilfield, Iraq. J. Petrol. Sci. Eng. **171**, 1338–1349 (2018)
2. Al-Khdheeawi, E.A., Vialle, S., Barifcani, A., Sarmadivaleh, M., Iglauer, S.: Effect of wettability heterogeneity and reservoir temperature on CO2 storage efficiency in deep saline aquifers. Int. J. Greenhouse Gas Control **68**, 216–229 (2018)
3. Jodeyri-Agaii, R., Rahimpour-Bonab, H., Tavakoli, V., Kadkhodaie-Ilkhchi, R., Yousefpour, M.R.: Integrated approach for zonation of a mid-Cenomanian carbonate reservoir in a sequence stratigraphic framework. Geol. Acta **16** (2018)
4. Rosales, I., Pomar, L., Al-Awwad, S.F.: Microfacies, diagenesis and oil emplacement of the Upper Jurassic Arab-D carbonate reservoir in an oil field in central Saudi Arabia (Khurais complex). Marine Petrol. Geol. **96**, 551–576 (2018)
5. Zhang, P., Zhang, J., Wang, J., Li, M., Liang, J., Wu, Y.: Flow units classification for geostatisitical three-dimensional modeling of a non-marine sandstone reservoir: a case study from the Paleocene Funing Formation of the Gaoji Oilfield, east China. Open Geosci. **10**, 113–120 (2018)
6. Parvizi, H., Rezaei Gomari, S., Nabhani, F., Dehghan Monfared, A.: Modeling the risk of commercial failure for hydraulic fracturing projects due to reservoir heterogeneity. Energies **11**, 218 (2018)
7. Aghli, G., Moussavi-Harami, R., Mohammadian, R.: Reservoir heterogeneity and fracture parameter determination using electrical image logs and petrophysical data (a case study, carbonate Asmari Formation, Zagros Basin, SW Iran). Petrol. Sci. **17**, 51–69 (2019)
8. Yuan, B., Zhang, Z., Clarkson, C.R.: Improved distance-of-investigation model for rate-transient analysis in a heterogeneous unconventional reservoir with nonstatic properties. SPE J. **24**, 2362–2377 (2019)
9. Abdelwahhab, M.A., Raef, A.: Integrated reservoir and basin modeling in understanding the petroleum system and evaluating prospects: the Cenomanian reservoir, Bahariya Formation, at Falak Field, Shushan Basin, Western Desert, Egypt. J. Petrol. Sci. Eng. **189**, 107023 (2020)
10. Santoso, R., Torrealba, V., Hoteit, H.: Investigation of an improved polymer flooding scheme by compositionally-tuned slugs (2020)